PUBLICATIONS OF THE ASTRONOMICAL SOCIETY OF THE PACIFIC, **114**:577–585, 2002 May
© 2002. The Astronomical Society of the Pacific. All rights reserved. Printed in U.S.A.

Building a CCD Spectrograph for Educational or Amateur Astronomy

SHEILA J. KANNAPPAN,[1,2] DANIEL G. FABRICANT,[1] AND CHARLES B. HUGHES[1]
Received 2002 January 23; accepted 2002 February 11

ABSTRACT. We discuss the design of an inexpensive, high-throughput CCD spectrograph for a small telescope. By using optical fibers to carry the light from the telescope focus to a tabletop spectrograph, one can minimize the weight carried by the telescope and simplify the spectrograph design. We recently employed this approach in the construction of IntroSpec, an instrument built for the 16 inch Knowles Telescope on the Harvard College campus.

1. INTRODUCTION

The widespread availability of affordable, high-quality commercial CCD cameras for astronomy now makes it possible for educators and amateur astronomers to conduct sophisticated observing programs with small telescopes and limited resources. In recent years the potential for building inexpensive CCD spectrographs around these cameras has been recognized by several companies and individuals (e.g., Glumac & Sivo 1999). Observations of the spectra of stars, planets, and nebulae open up an exciting new realm of inquiry for beginning astronomers, and the design and construction of the spectrograph itself can provide students with a hands-on education in the principles of optics and engineering. Here we describe one approach to designing and building a simple CCD spectrograph, based on IntroSpec, an educational instrument we recently built for the Harvard Astronomy Department.

We had four design goals for IntroSpec: (1) sufficient spectral range and resolution for a variety of projects in optical astronomy, (2) high throughput to enable observations of nearby nebulae and variable stars, (3) simple controls and a durable design suitable for student operation, and (4) a small telescope-borne weight. We decided on a spectral range of ~4500–6800 Å at ~6 Å resolution. This wavelength range includes many important spectral features: H, Fe, Mg, and Na absorption lines (prominent in stellar atmospheres), molecular absorption bands from CH_4 and NH_3 (visible in planetary atmospheres), as well as H, N, and O emission lines (characteristic of star-forming nebulae). Spectral coverage extending ~1000 Å farther to the blue would be useful, but most inexpensive CCD chips have poor UV response. Our chosen resolution of 6 Å allows detection of most of the commonly observed features in this spectral range and is adequate to resolve the closely spaced emission lines of Hα and [N II].

We were able to meet our design goals on a budget of slightly under $5500, of which ~$4000 went into buying a midrange Meade CCD camera and paying for the time and materials of a skilled machinist (C. B. H.).[3] Below we describe how IntroSpec's design was tailored to the specific challenges posed by our budget and performance requirements. Section 2 reviews the general optical design constraints on any similar spectrograph, while § 3 examines the specific choices we made for IntroSpec, with special attention to the instrument's fiber-fed design.

2. OPTICAL DESIGN

We begin with a brief review of the layout of a generic spectrograph, then consider how to optimize its optical design.

2.1. Layout of a Generic Spectrograph

Figure 1 shows the light path in a simple CCD spectrograph. The aperture accepts light from a small portion of the telescope focal plane that may contain the image of a star or a portion of an extended nebula. This light is collimated with a lens, producing a parallel beam. The beam travels to a diffraction grating, which disperses the light into a spectrum described by the grating equation (e.g., Schroeder 2000)

$$m\lambda = d(\sin\theta_1 + \sin\theta_2), \quad (1)$$

where m is the diffraction order, λ is the wavelength of the light, d is the grating line spacing, and θ_1 and θ_2 are the incoming and outgoing angles of the light with respect to the normal to the grating surface (see Schroeder for sign conventions).

A reflection grating such as that shown in Figure 1 folds the light path as well as dispersing the light. In this case the angle

[1] Harvard-Smithsonian Center for Astrophysics, 60 Garden Street MS-20, Cambridge, MA 02138; skannappan@cfa.harvard.edu, dfabricant@cfa.harvard.edu, cn0412@hotmail.com.

[2] Present address: University of Texas at Austin, McDonald Observatory, 2511 Speedway, RLM 15.308 C1400, Austin, TX 78712; sheila@astro.as.utexas.edu.

[3] These numbers do not include an expensive but desirable accessory: a Hg-Ne lamp for wavelength calibration. We purchased one from Oriel for an additional $450.

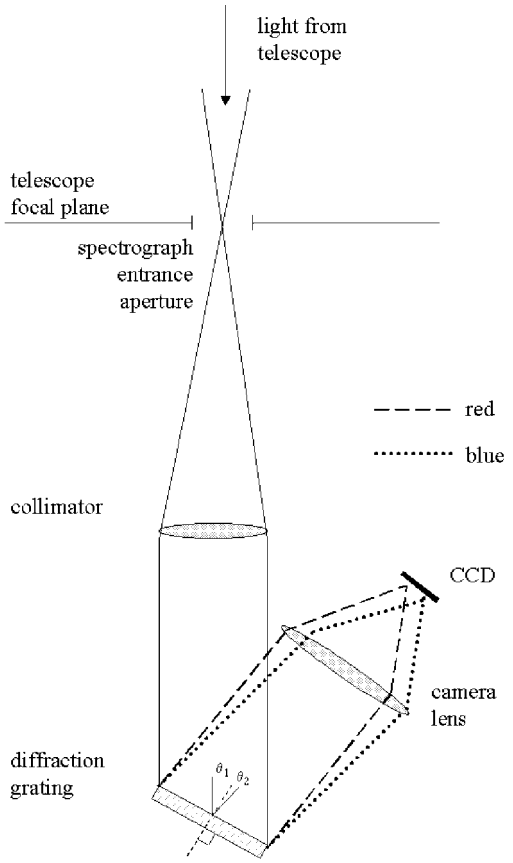

FIG. 1.—Schematic of the optics in a simple spectrograph with a reflection grating. Because the angle between the grating normal and the camera's optical axis (θ_2) is smaller than the angle between the grating normal and the collimator's optical axis (θ_1), the diameter of the monochromatic collimated beam leaving the grating has a larger diameter than the incident beam (anamorphic magnification).

between the incident and diffracted beam typically must be greater than 30° to allow the camera optics to stay clear of the collimated beam heading toward the grating. The grating normal generally points closer to the camera axis than to the collimator axis (Schroeder 2000), leading to anamorphic magnification: a geometrical expansion of the dispersed collimated beam along the dispersion axis described by $\mathrm{AM} = \cos\theta_2/\cos\theta_1$ (see Fig. 1). Anamorphic magnification increases the spectral resolution by the same factor that the collimated beam is expanded but requires a larger camera acceptance aperture to avoid vignetting. Camera-collimator angles exceeding 45° are rarely used for this reason.

The light dispersed by the grating is a superposition of collimated beams of different colors, all traveling at slightly different angles. The camera lens focuses each color onto a location on the CCD chip determined by its incoming angle, thereby forming a spectrum. This focusing process is exactly analogous to the way a telescope focuses incoming parallel light beams from stars at different angles on the sky onto different positions on the telescope focal plane: in the spectrograph, each point along the spectrum is an image of the light from the spectrograph entrance aperture at a different wavelength. A higher dispersion grating increases the angular spread between collimated beams of different colors, spreading the corresponding images farther apart. For a detector of fixed size, higher dispersion yields higher spectral resolution at the expense of reduced spectral coverage.

2.2. Setting the Relative Scales of the System

Independent of the grating choice or the absolute scale of the spectrograph, we wish to specify the relative focal lengths of the spectrograph optics so that the image of the spectrograph entrance aperture is correctly sampled by the CCD pixels. The width of this image in the dispersion direction defines the spectroscopic resolution element. Oversampling the image wastes CCD pixels and decreases spectral coverage, while undersampling it degrades spectral resolution. In the Nyquist sampling limit, ~2 pixels per wavelength allow one to recover the peak and valley of an oscillating waveform. Typically, finer sampling up to 3–4 pixels per resolution element is advantageous in professional instruments with large CCD chips. However, for an economical instrument, CCD pixels for spectral coverage are at a premium, and one may prefer sampling near the Nyquist limit. With Nyquist sampling, IntroSpec's design target of 6 Å resolution combined with 2300 Å spectral coverage requires a CCD chip with $2 \times 2300/6 = 767$ pixels. We chose this combination of spectral resolution and spectral coverage knowing that the largest CCD within our budget had 768 pixels in the long dimension.

Once the desired sampling is chosen, the ratio of the focal lengths of the collimator and camera lenses, f_{coll} and f_{cam}, is determined by the diameter ratio of the spectrograph entrance aperture and its image. For Nyquist sampling, the image of the spectrograph entrance aperture must be reduced to ~2 CCD pixels, or ~20 μm for a typical amateur CCD camera. The spectrograph entrance aperture has generally been sized to the expected diameter of a stellar image at the telescope's focus, which is determined by atmospheric conditions and the telescope optics. This choice maximizes the contrast between the object and the background sky light. For the 40 cm f/10 Knowles Telescope at Harvard, the local 5″ seeing disk makes a 100 μm image at the telescope's focus, implying that $f_{\mathrm{coll}}/f_{\mathrm{cam}}$ must equal ~5 to reduce the image to ~20 μm. For a 20 cm f/10 telescope, similar seeing would make a 50 μm point-source image, requiring an $f_{\mathrm{coll}}/f_{\mathrm{cam}}$ ratio of ~2.5. However, a larger entrance aperture (implying higher $f_{\mathrm{coll}}/f_{\mathrm{cam}}$ to achieve the same resolution) might be desirable for a 20 cm telescope to allow for image shifts due to imperfect guiding.

The acceptance angles of the collimator and camera lenses can also be estimated approximately independently of the absolute scale of the spectrograph. The collimator must be fast enough to accept an f/10 light cone from the telescope from

TABLE 1
CHOOSING THE CAMERA LENS AND DIFFRACTION GRATING

Camera Focal Length (mm)	Collimator Focal Length (mm)	Collimated Beam Diameter[a] (mm)	Grating Ruling Density[b] (lines mm^{-1})	Spectral Range[c] (Å)	2 Pixel Spectral Resolution (Å)	Anamorphic Magnification
35	175	17.5	900	2161	5.6	1.20
50	250	25.0	600	2267	5.9	1.13
85	425	42.5	300	2636	6.9	1.06

[a] The clear apertures of the optical elements must be larger than the nominal collimated beam diameter for the reasons discussed in § 2.2.

[b] Commonly available grating ruling closest to the ideal grating ruling for the indicated f_{cam}. The ideal value may be estimated to within ~5% from $\Delta\theta/\Delta\lambda_{spec}$, where $\Delta\theta$ is the angular diameter of the CCD chip at f_{cam} (in radians) and $\Delta\lambda_{spec}$ is the preferred wavelength resolution (in millimeters). We assume that the grating is used in first order.

[c] Spectral range calculated by determining the wavelength falling at each end of the CCD chip, using the grating equation.

every point within the spectrograph entrance aperture. This aperture typically takes the form of a long slit to enable spatial sampling perpendicular to the dispersion direction. The camera must be faster than the collimator: if $f_{coll}/f_{cam} \sim 5$, each monochromatic beam intercepted by the camera has a focal ratio of ~f/2 and is elongated in the dispersion direction by anamorphic magnification (see § 2.1). These beams must be accepted over a field of view that is extended in both the spatial direction (because of the slit length) and the dispersion direction (because of the angular divergence of the different wavelengths in the spectrum; § 3.3).

2.3. Setting the Absolute Scale of the System

We have some flexibility in choosing the overall dimensions of the optics, limited by financial constraints and the desired spectroscopic performance. We must balance two considerations. First, larger optics and their mounts are generally more expensive, although the economies of mass-produced commercial optics can bend this rule. Second, to maintain a given spectral range and resolution on a fixed CCD format, one must keep the product of the grating dispersion (ruling density) and the focal length of the camera constant. The grating cost goes up nonlinearly with the ruling density, so the grating cost and availability must be balanced against the cost of the optics, particularly the camera lens.

The widespread availability of commercial 35 mm format single lens reflex (SLR) photographic lenses suggests an attractive solution. These lenses are inexpensive, offer excellent image quality, have sophisticated antireflection coatings, and are designed to work over a film format of 24 × 36 mm. CCD chips in typical amateur cameras fit easily within this format. Many photographic lenses can produce images of ~20 μm diameter, or about 2 pixels for a CCD camera with ~10 μm pixels. Excellent used lenses can be obtained for less than $100, particularly if an older manual focus lens is selected.

To minimize vignetting, our design for IntroSpec calls for a camera lens faster than f/2 (§ 2.2), so an f/1.4 lens is a good choice. Commercial 35 mm SLR lenses as fast as f/1.4 are typically available with focal lengths between 35 and 85 mm, with 50 mm being by far the most common. These focal lengths pair conveniently with readily available diffraction gratings to meet our goals for spectral coverage and resolution. Table 1 describes three combinations of gratings and lenses with focal lengths between 35 and 85 mm. We assume a camera-collimator angle of 36°, a central wavelength of 5650 Å, and a 6.9 mm CCD chip with 768 pixels (as found in IntroSpec). All of these lens-grating combinations approximately satisfy our design targets of 6 Å resolution and 2300 Å spectral coverage. Given the ease of obtaining both 50 mm focal length lenses and 600 line mm^{-1} gratings, we selected this configuration for IntroSpec. The spectrograph would have been somewhat smaller had we used a more expensive 35 mm focal length camera lens, but as Table 1 demonstrates, vignetting due to anamorphic magnification would be slightly greater.

3. INTROSPEC

3.1. Optical Fibers Ease Design Constraints

IntroSpec's design follows that of the generic CCD spectrograph in Figure 1, with one key difference: the spectrograph does not mount directly to the telescope. This change reflects the optical design constraints outlined in § 2, which led us to prefer moderately large optical elements (a 50 mm focal length camera lens and a 250 mm focal length collimator), implying an instrument whose longest dimension exceeds 0.5 m. A commercial 40 cm telescope can support neither the size nor the weight of such an instrument. Instead of sacrificing optical performance, we opted for a bench-mounted, fiber-fed design. Light from the telescope enters a set of optical fibers at the telescope's focus, and from there the fibers carry the light to IntroSpec, which sits on a table. Because IntroSpec's weight is removed from the telescope, it can be packaged in a heavy metal box with an easy-to-remove lid, which protects the instrument while keeping it accessible to students. IntroSpec's wavelength calibration is stable because the mechanical flexure encountered in a telescope-mounted spectrograph is eliminated.

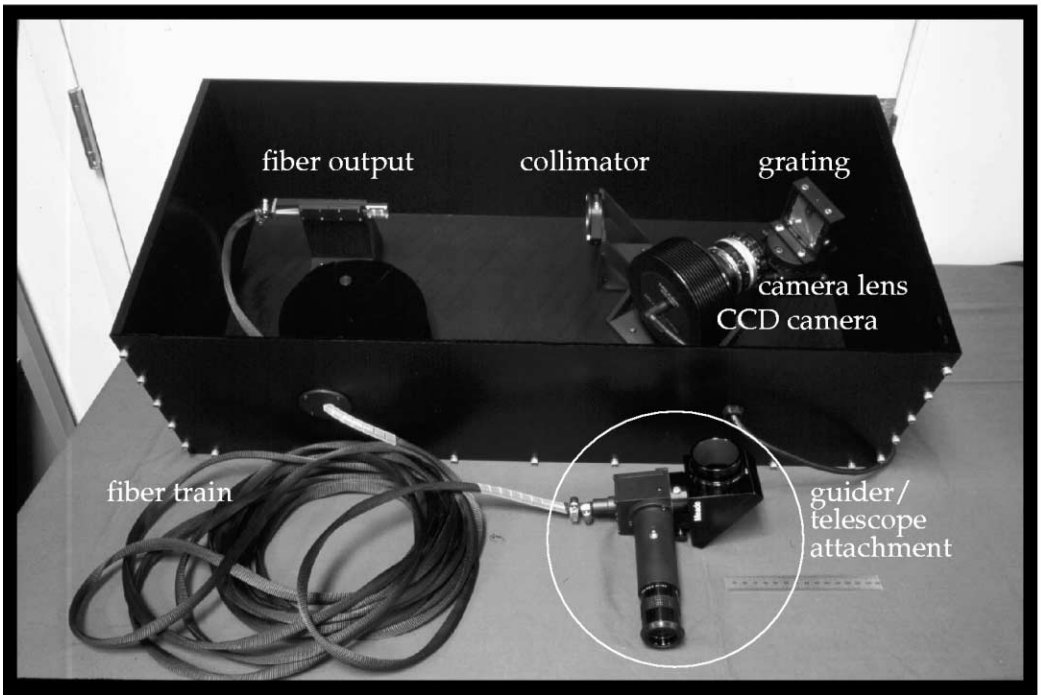

FIG. 2.—Overview of IntroSpec. See § 3.2 and Table 2.

3.2. General Overview of the Instrument

Figure 2 and Table 2 provide an overview of IntroSpec. Optical fibers are coupled to the telescope via a guider/telescope attachment, further discussed in § 3.6. The fiber train consists of six fibers, each of which accepts light from a different position on the telescope focal plane; these are bundled in several layers of protective coverings. (Section 3.4 discusses the technical aspects of working with fibers in more detail.) Upon entering the spectrograph enclosure, the fiber train loops around a large black spool for strain relief; then the fibers are channeled into the fiber output, from which the bare fiber ends emerge in a vertical stack (Fig. 3). The base of the fiber output assembly is adjustable to permit focusing the collimator lens. Each optical fiber is an independent spectrograph entrance aperture; by stacking these apertures perpendicular to the dispersion axis, we obtain six parallel spectra on the CCD chip (Fig. 4).

IntroSpec uses two fibers of each of three diameters: 100, 200, and 300 μm. The seeing disk at the Knowles telescope is well matched to a 100 μm fiber, and this fiber diameter provides the highest spectral resolution, ~6 Å FWHM. Larger fibers give the user the choice of trading off spectral resolution in exchange for gathering additional light from an extended source such as a nebula. Larger fibers are also more forgiving of guiding errors when spectral resolution is not critical. The different fiber diameters allow students to learn about the instrument and to make the connection between fiber size and spectral resolution. For point sources, one fiber can be used to acquire the target spectrum and the second fiber of the same diameter can be used to acquire a sky spectrum for background subtraction.

From the collimator on, IntroSpec looks much like the generic spectrograph of Figure 1. The collimator lens is a 50 mm diameter achromat with $f_{\rm coll} = 250$ mm, yielding a collimated beam diameter of 25 mm with an f/10 input light cone. We selected a 588 line mm^{-1} grating blazed[4] for peak efficiency at 5610 Å. Richardson Grating Laboratory offers this grating in sizes up to ~50 mm square. The grating face is precisely aligned to the rotation axis of a rotation stage, permitting micrometer adjustment of the grating angle to vary the spectral range. With a camera-collimator angle of 36°, IntroSpec's design range of 4500–6800 Å corresponds to an 8° angle between the grating normal and the camera axis. At this rotation angle, the anamorphic magnification factor is 1.1, so the monochromatic outgoing beams are oval in shape with dimensions ~25 × 28 mm.

These beams travel ~90 mm from the grating to the camera lens, where the dispersed colors slightly overfill the 38 mm

[4] The ruled diffraction gratings typically used in astronomical instruments are blazed to maximize the amount of light in the desired diffraction order. A blazed reflection grating has a triangular groove profile, with the reflective surface of the groove inclined to the grating surface by an angle known as the blaze angle. The blaze angle is chosen such that simple geometrical reflection from the groove face sends light not into the central maximum but instead into the chosen diffraction order, coincident with the desired peak-efficiency wavelength. In the case of transmission gratings, the blaze angle is chosen such that light geometrically refracted from the groove face is coincident with the desired peak-efficiency wavelength in the selected diffraction order. We chose a reflection grating for IntroSpec because reflection gratings are somewhat less expensive than transmission gratings and the folding of the light path is convenient.

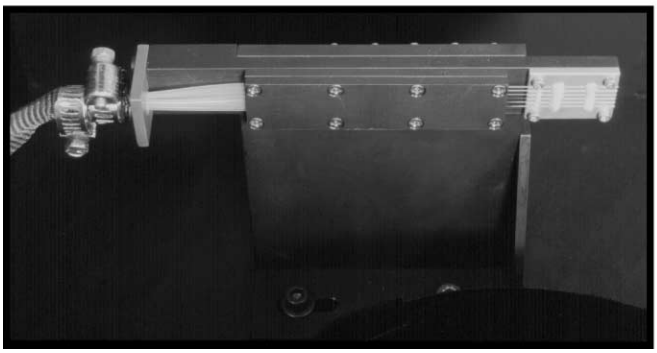

FIG. 3.—Fiber output assembly. Three pairs of fibers with diameters of 100, 200, and 300 μm are arranged vertically, with the smallest fibers at the center and the largest fibers at the top and bottom. The ends of the fibers are aligned precisely in six V-grooves; the V-grooves are bead blasted but not anodized (see § 3.4).

maximum aperture of the camera lens, a 50 mm focal length f/1.4 Nikon lens (see the discussion of vignetting in § 3.3). The lens focuses the spectrum onto a Meade Pictor 416 XT CCD camera, containing a 768 × 512 KAF-0400 chip with 9 μm square pixels. Attaching the Nikon lens to the Pictor 416 XT required machining a special connector made from a Nikon bayonet mount and a Meade CCD camera mount. Finally, the cord shown exiting the spectrograph enclosure to the front right in Figure 2 connects the CCD camera to the Meade Pictor control box (not shown) for data and power transfer.

3.3. Image Quality and Vignetting

We have modeled IntroSpec's optical performance using the commercially available optical design and analysis code ZEMAX. The optical prescription for the collimator achromat is included in the lens catalog supplied with ZEMAX. The precise optical prescription for the Nikon lens is not available, so for this lens we have substituted the scaled prescription for a 100 mm focal length, f/1.4 double Gauss lens from a compilation of lens designs by Smith (1992). The Nikon lens used in IntroSpec is also of the double Gauss design and should perform similarly.

Our ray traces for the model IntroSpec give images with rms image diameters between 12 and 30 μm across the target 4500–6800 Å wavelength range when the camera lens is stopped down to f/1.8. The performance is considerably worse when the lens is opened to its full f/1.4 aperture. Our laboratory tests show that the actual Nikon lens produces CCD images with FWHM diameters of ~20–25 μm when the grating is illuminated with collimated light, in good agreement with the ray traces.

Our ray traces also allow us to estimate the vignetting in the camera lens as a function of wavelength. As shown in Figure 5, when the camera lens is stopped down to f/1.8, the on-axis (5650 Å) beam is unvignetted, and ~68% of the extreme (4500 or 6800 Å) beams are transmitted.

3.4. Throughput and Optical Fiber Losses

We estimate IntroSpec's total throughput at about 12% at 5650 Å. Throughput is lower at the ends of the spectral range because of vignetting in the camera lens, the decrease of the grating efficiency off the blaze peak, and the wavelength dependence of the quantum efficiency of the CCD camera.

Table 3 lists the individual throughput of each of IntroSpec's optical elements, not including losses due to guiding errors or the finite apertures of the fibers. With high-quality components,

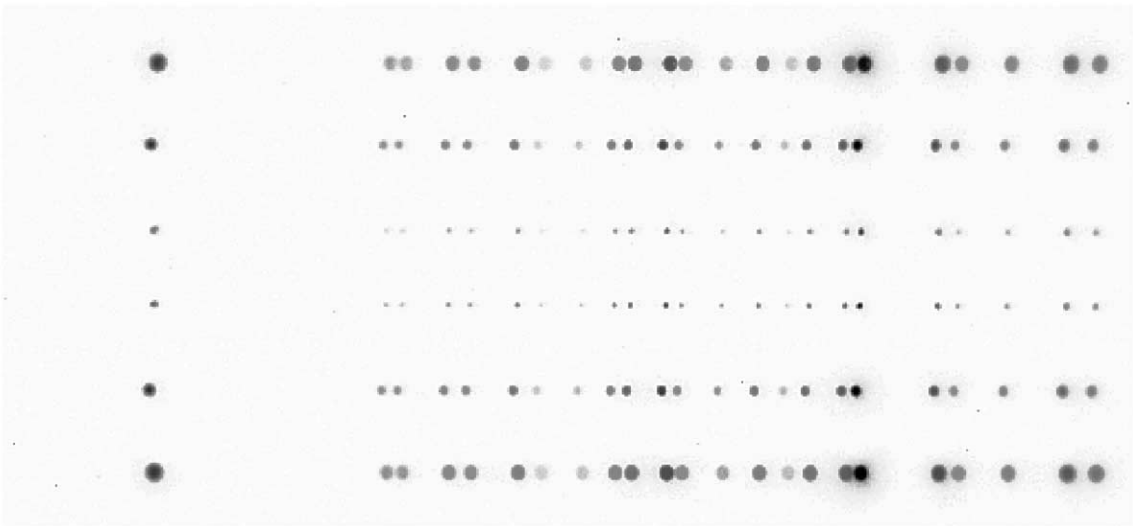

FIG. 4.—CCD image of spectra from IntroSpec's six optical fibers. The fibers have been illuminated with a mercury-neon calibration lamp, which emits a number of narrow emission lines. Here the camera lens was opened all the way to f/1.4, and a small amount of light in a diffuse halo is visible surrounding the brighter lines.

TABLE 2
PURCHASED PARTS LIST

Spectrograph
Newport PAC088 cemented achromat, 2 inch diameter, $f = 250$ mm
Newport LH-200 2 inch diameter lens mount
Richardson Grating Lab 588 line mm^{-1} reflection grating, 50 × 50 × 6 mm blazed at 561 nm
Newport 481-A Rotation Stage
Nikon f/1.4 $f = 50$ mm photographic lens
Meade Pictor 416 XT CCD camera
Meade 12 V DC to 115 AC adapter
1.25 inch CCD barrel from Meade Customer Service
Surplus bayonet mount (free from photography shop)
Guider
Two Newport PAC040 precision achromatic doublets, 25.4 mm diameter, EFL = 50.8 mm
Orion Sirius Plossl eyepiece, 1.25 inch diameter, $f = 26$ mm
Meade 2 inch diagonal mirror No. 929
Fiber Train
Polymicro FVP series multimode step-index fiber, core diameter 100 and 300 μm
Fiberguide SFS200 240T multimode step-index fiber, core diameter 200 μm
M M Newman 20 gauge PTFE standard wall Teflon tubing
Bally Ribbon Mills Pattern 8444 0.5 inch tubular nylon webbing

NOTE.—All other parts were made in the machine shop or the lab.

the lens and grating efficiencies are hard to improve. However, current versions of the Meade Pictor CCD cameras use CCDs that have quantum efficiencies of ~50% at 5650 Å, noticeably higher than the 35% quantum efficiency of the older model in IntroSpec.

Achieving the optical fiber throughput shown in Table 3 requires some attention to minimizing fiber losses. IntroSpec uses multimode, step-index fibers with a pure fused silica core and doped fused silica cladding because this type of fiber provides the best overall throughput for the wavelengths of interest in astronomical spectroscopy.

Fiber losses come from three main sources: end reflection losses, internal transmission losses, and focal ratio degradation. End reflection losses are simply the Fresnel reflection losses encountered at every material interface; for fused silica, the refractive index is ~1.46 at the center of the IntroSpec passband, resulting in a loss of ~3.5% at each fiber end. These losses are hard to avoid because it is usually not practical to apply antireflection coatings to the tiny fiber ends. Internal transmission losses can be estimated using data from the fiber manufacturer and vary according to the OH content of the fused silica and the material preparation. For the 10 m long fibers used in IntroSpec, internal transmission losses are negligible in the 4500–6800 Å range, although transmission losses become more important below 4000 Å. A discussion of the internal transmission of modern fused silica fibers can be found in Lu et al. (1998).

TABLE 3
ESTIMATED INTROSPEC THROUGHPUT AT 5650 Å

Optical Element	Transmission
Fibers	0.60
Collimator lens	0.97
Grating	0.70
Camera lens	0.86
CCD	0.35
Total throughput	0.12

Focal ratio degradation is the major controllable source of fiber losses. If a fiber is manufactured to high standards and not pinched in use, a light cone incident on the fiber axis exits the fiber with approximately the same focal ratio with which it entered. (The fibers we have chosen accept a numerical aperture of 0.22, corresponding to a focal ratio of ~f/2.2, much faster than the required f/10.) However, stresses that locally deform the fiber will scatter light into a faster cone, resulting in focal ratio degradation. This degradation in turn leads to reduced system throughput if the optics are not enlarged to capture the faster cone of light. Our tests have shown that even if fibers are carefully mounted, protected from stress, and properly aligned, focal ratio degradation will scatter about 25% of the light incident at f/10 outside an f/10 light cone. Accounting for reflection losses at both ends of the fiber, the total fiber throughput under ideal conditions is then about 70% at f/10. Focal ratio degradation is much less important for input beams significantly faster than f/10. We recommend avoiding fibers with core diameters smaller than 100 μm because they are more difficult to handle and are more prone to focal ratio degradation.

3.5. Mounting Optical Fibers

The most common source of excess focal ratio degradation is external stress due to inappropriate fiber mounting tech-

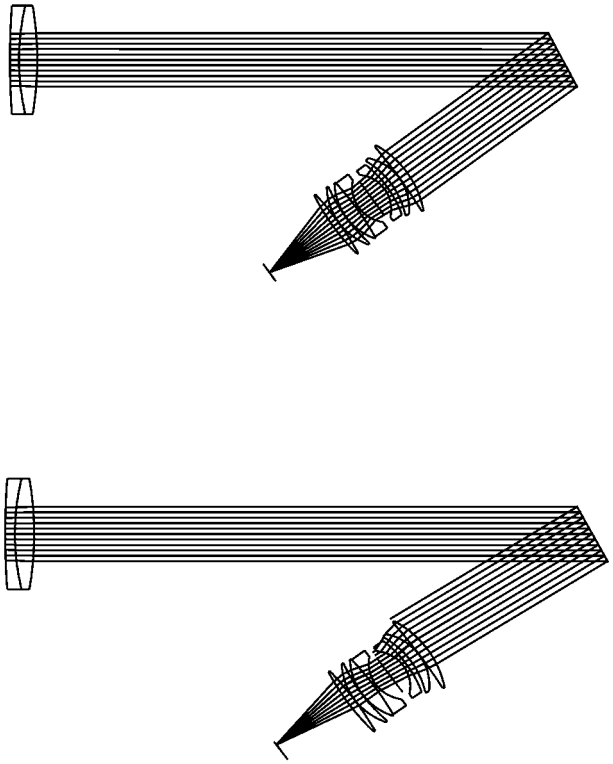

FIG. 5.—Optical light path from the collimator to the focal surface for two wavelengths, near 5650 Å in the top panel and near 6800 Å in the bottom panel. The camera lens is stopped down to f/1.8. Approximately 32% of the light is lost to vignetting at 6800 Å.

niques. For example, if the fibers are bonded into an oversized ferrule with a circumferential epoxy bond, the epoxy shrinkage upon curing can introduce serious stress. A much better technique is to bond the fibers onto precisely machined V-grooves (long grooves with a V-shaped cross-sectional profile) with small beads of silica-filled epoxy. Mixing epoxy and silica half and half by weight reduces the epoxy shrinkage, and the viscous mixture does not completely surround the fiber (Fig. 3).

To machine the V-grooves, we use a 45° double angle cutter in an R-8 or 3/4 inch straight shank stub milling machine arbor. Cutters with noticeable radii on the cutting teeth should be avoided, because a large radius will disturb the fiber alignment by allowing the fiber to contact the groove bottom. After the grooves are cut, we lightly bead blast them with glass beads; this process removes burrs that may stress or scratch the fibers and also creates a good surface for bonding.

Stress along the length of the fiber can be minimized by enclosing each fiber in a loosely fitting sleeve of Teflon tubing (in addition to any plastic buffer the fiber may already be coated with); for convenience and extra protection, we also bundle these tubes within a larger fabric sheath. Several stages of strain relief at both ends of the fiber train protect the fibers from accidental tugs and maintain a large bend radius.

Accurate fiber alignment and polishing is also critical, to avoid both focal ratio degradation losses at the entrance fiber face and misdirection of the exiting light at the exit fiber face. Both the entrance and exit ends of the fibers must be polished flat to a good optical finish, and the polished ends must be perpendicular to the fiber axes (which are aligned perpendicular to the focal plane using the precisely machined V-grooves). We used a fiber-polishing machine built for an earlier project; a similar machine could be constructed for ~$300 in parts. The machine consists of a flat glass disk attached to an aluminum turntable rotating on a 72 revolution per minute motor. A rigid arm holds a brass cylinder perpendicular to the glass disk. The brass cylinder has V-grooves cut along its length, and the fibers are temporarily attached to the V-grooves with Duco cement for polishing. A large drop of Duco cement covers the end of each fiber, which protrudes by ~2 mm (most of this will be polished away). We attach disks of high-quality self-adhesive abrasive paper in successively finer grades to the turntable, and the brass cylinder containing the fibers is swept across the abrasive paper. The sequence begins with 30 μm grit paper and ends with 0.3 μm grit paper. A thin solution of dishwashing soap in water provides adequate lubrication; clean water is used to rinse off grit residue before moving to the next smaller grit (the motor is isolated from water spills). Finally, we inspect the fiber ends under a microscope to verify that no scratches remain. The Duco cement can be removed with acetone to release the fiber from the polishing cylinder.

3.6. The Manual Guider

Acquiring and tracking astronomical targets requires some technique for viewing the focal plane. In a professional instrument this function is usually performed by a sensitive, high frame rate electronic camera. In IntroSpec we have provided optics that allow the observer to visually monitor and correct the telescope tracking while viewing a 12′ field of view imaged around the spectrograph entrance aperture.

Figure 6 illustrates the primary components of the guider. A flat metal mirror intersects the focal plane of the telescope at a 45° angle. The mirror is machined in two pieces, and the fibers protrude through the mirror at the intersection of the focal plane and the mirror's surface. All the light that does not enter the fibers strikes the mirror and is reflected by 90° into the eyepiece extension. Inside the extension, two matched achromatic lenses relay the image of the telescope focal plane to a 26 mm Plossl eyepiece. The observer guides the telescope by centering the object of interest on one of the fiber ends so that most of the light disappears down the fiber.

The guider also serves as the mechanical interface between the telescope and the fibers, incorporating mechanisms for eye-

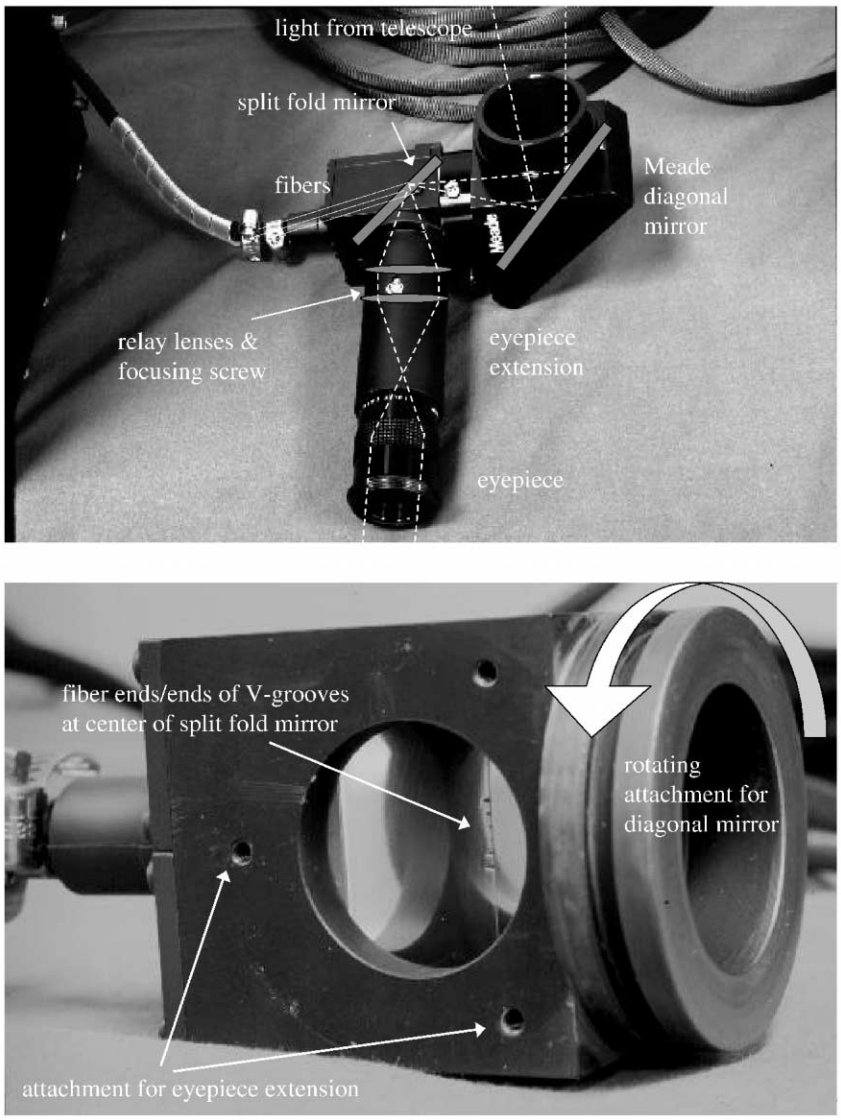

FIG. 6.—Guider/telescope attachment. *Top:* Lines drawn over the photo show the positions of the optical components and the path of the light. The small screw between the relay lenses allows them to slide forward or backward as a unit to focus. *Bottom:* Inner guider assembly, with the Meade diagonal mirror and the eyepiece extension removed to reveal the split mirror in the central piece. The fibers are not easily visible in the photo, but they protrude slightly from the V-grooves, with their polished surfaces flush to the focal plane of the telescope (i.e., at a 45° angle from the mirror surface).

piece rotation, strain relief, and fiber alignment. To minimize weight, nearly all of the parts were made from aluminum, including the mirror. We finished the mirror in two steps, first removing machining marks with a fine grit paste on a turntable and then polishing with white rouge compound and a hard felt wheel mounted on a lathe. The two halves of the mirror were registered with pins, allowing us to disassemble the mirror to mount the fibers in internal V-grooves without disturbing the polished surface.

4. CONCLUSION

IntroSpec saw first light on 1999 March 17 and is now in regular use in a Harvard astronomy course for nonmajors. Students perform projects such as comparing the spectra of the two stars in Albireo. Even under a bright urban sky, we have successfully used IntroSpec to observe objects ranging from stars and planets to emission nebulae and binary accretion systems. Figure 7 shows a few spectra taken with IntroSpec along

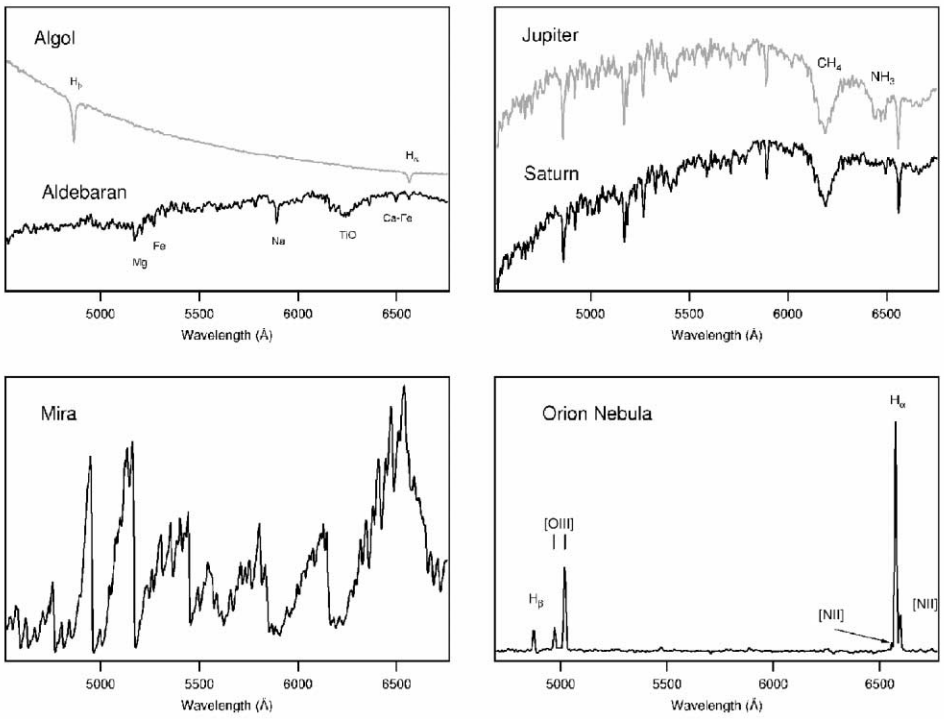

FIG. 7.—Spectra taken with IntroSpec at the Knowles Telescope. Approximate exposure times: Algol 30 s, Aldebaran 3 s, Jupiter 3 s, Saturn 6 s, Mira 30 s, and Orion Nebula 600 s. Observations were taken on different nights with variable (but never photometric) sky conditions. All spectra except Orion were taken with the 100 μm fiber for maximum spectral resolution (~6 Å); for Orion we binned the CCD by 2 but still used the 100 μm fiber because of readout glitches in the 200 μm fiber spectrum. The resulting spectral resolution of ~12 Å just suffices to distinguish the N II line at 6548 Å from Hα at 6563 Å. The sawtooth structure in Mira's spectrum is caused by absorption bands of TiO and other molecules in its outer envelope.

with their exposure times. We have also used IntroSpec to demonstrate to students how a spectrograph works; the instrument's easy-to-remove top cover allows students to peer directly inside. In another article (Kannappan & Fabricant 2000) we provide a brief introduction to amateur spectroscopy with low-budget spectrographs like IntroSpec, including basics of data analysis and interpretation as well as a variety of spectroscopy project ideas.

IntroSpec was designed and built at the Harvard-Smithsonian Center for Astrophysics, with financial support from Harvard College and the Harvard Astronomy Department arranged by Jonathan Grindlay and Ramesh Narayan. We thank Professor Grindlay for his participation in planning and commissioning the instrument. The Knowles Telescope where IntroSpec is used was generously donated by C. Harry and Janet Knowles. We are grateful to John Geary, Steve Amado, Joe Zajac, Douglas Mar, John Roll, Warren Brown, and Anita Bowles for advice, resources, and technical assistance during IntroSpec's construction phase. We also thank Tom Narita, John Raymond, Dimitar Sasselov, and the students, friends, and family who helped with commissioning runs.

REFERENCES

Glumac, N., & Sivo, J. 1999, S&T, 97, 134
Kannappan, S., & Fabricant, D. 2000, S&T, 100, 125
Lu, G., Schoetz, G. F., Vydra, J., & Fabricant, D. 1998, Proc. SPIE, 3355, 884
Schroeder, D. J. 2000, Astronomical Optics (San Diego: Academic)
Smith, W. J. 1992, Modern Lens Design: A Resource Manual (New York: McGraw-Hill)